Cisplatin DNA damage and repair maps of the human genome at single-nucleotide resolution

Jinchuan Hu[a], Jason D. Lieb[b], Aziz Sancar[a,1], and Sheera Adar[a,1]

[a]Department of Biochemistry and Biophysics, University of North Carolina School of Medicine, Chapel Hill, NC 27599-7260; and [b]Department of Biology, University of North Carolina at Chapel Hill, Chapel Hill, NC 27599

Contributed by Aziz Sancar, August 31, 2016 (sent for review August 4, 2016; reviewed by Michael Leffak and Pengbo Zhou)

Cisplatin is a major anticancer drug that kills cancer cells by damaging their DNA. Cancer cells cope with the drug by removal of the damages with nucleotide excision repair. We have developed methods to measure cisplatin adduct formation and its repair at single-nucleotide resolution. "Damage-seq" relies on the replication-blocking properties of the bulky base lesions to precisely map their location. "XR-seq" independently maps the removal of these damages by capturing and sequencing the excised oligomer released during repair. The damage and repair maps we generated reveal that damage distribution is essentially uniform and is dictated mostly by the underlying sequence. In contrast, cisplatin repair is heterogeneous in the genome and is affected by multiple factors including transcription and chromatin states. Thus, the overall effect of damages in the genome is primarily driven not by damage formation but by the repair efficiency. The combination of the Damage-seq and XR-seq methods has the potential for developing novel cancer therapeutic strategies.

Damage-seq | XR-seq | nucleotide excision repair | cancer | chemotherapy

Cisplatin [Cis-diamminedichloroplatinum(II)] is a major frontline drug in the treatment of lung, colorectal, ovarian, and head-and-neck cancers (1) and has been used in the clinic since 1978. It kills cancer cells by damaging their DNA, mainly by forming Pt-d(GpG) and, to a lesser extent, Pt-d(ApG), Pt-d(GpXpG) intrastrand diadduct, and at lower frequency, Pt-G-G interstrand cross-links (2–4). The cisplatin-induced damage is repaired by nucleotide excision repair (5–8). In excision repair, the damage in DNA is excised from the genome as a single-stranded oligomer of ~30 nt. The single-stranded gap in the genome is filled in by DNA polymerases and ligated, resulting in error-free repair. Although cisplatin is effective in the treatment of the indicated types of cancers, in some of the cases, drug resistance is observed. The cause of the resistance is multifactorial, and DNA repair is considered to be one of the contributing factors, although the degree to which DNA repair contributes to resistance is still unclear. Here, we describe the development of methods to measure cisplatin adduct formation and repair at single-nucleotide resolution. Using these methods, named "Damage-seq" and "eXcision Repair-seq" (XR-seq), we have generated single-nucleotide resolution maps for both the damage induced by cisplatin and its removal by nucleotide excision repair (9, 10). Our method should be applicable for studying drug resistance and for optimization of cancer chemotherapy regimens.

Results

In this work, we present the cisplatin damage and repair maps for the entire genome of the human lymphocyte cell line GM12878. This cell line was chosen because it has been extensively characterized by the ENCODE project (11). Similar experiments with oxaliplatin, a third generation derivative of cisplatin, yielded similar results and are presented in *SI Appendix, SI Materials and Methods*. All experiments were performed with two biological replicates.

Cisplatin DNA Damage Map. We developed the method of Damage-seq based on the fact that bulky DNA adducts block high-fidelity DNA polymerases (2, 12). Here, we have applied Damage-seq to construct a human genome DNA damage map for cisplatin-induced damage. In Damage-seq (Fig. 1*A* and *SI Appendix*, Fig. S1), cells were treated with cisplatin and the genomic DNA was isolated and fragmented by sonication. Then the fragment ends were repaired, followed by ligation of the first adapter. Next, the DNA was denatured and immunoprecipitated with anti-Pt antibodies to isolate the ssDNA fragments containing the Pt adduct. Then, a biotinylated primer was annealed to the adapter and extended by NEBNext Q5 DNA polymerase. The extended primers were purified by streptavidin-coated beads. The second adapter was then ligated, followed by PCR with index primers. To check the quality of the libraries, 1% of the ligation products were amplified by two sets of primers corresponding to the first or second adapters and analyzed on agarose gels (Fig. 1*B* and *SI Appendix*, Fig. S2*A*). The first primer set supports amplification of only unblocked extension products from the undamaged strand, whereas the second set of primers amplifies all products from both damaged and undamaged strands. If the majority products came from the damaged strands, PCR products by the second primer set would be shorter and at a much higher level than those by the first primer set, which can only generate products from undamaged strands (Fig. 1*B*, compare lanes 2 and 4, and *SI Appendix*, Fig. S2*A*). In contrast, if most of the PCR products came from undamaged strands, the second set of primers would generate slightly longer PCR products (Fig. 1*B*, compare lanes 1 and 3). After sequencing,

Significance

The chemotherapy drug cisplatin kills cancer cells by damaging their DNA. It has been used for treating a variety of cancer types for almost four decades. Although the drug is generally effective, it has strong adverse side effects, and some cancers exhibit or, after initial favorable response, develop drug resistance. The mechanism of drug resistance is multifactorial and involves the ability of cancer cells to repair the cisplatin-induced DNA damages. We have developed methods to map the sites of cisplatin damage and its repair for the entire human genome at single-nucleotide resolution. These methods can be used to study cancer sensitivity and resistance to the drugs, and to identify new strategies for efficient combination therapies.

Author contributions: J.H., J.D.L., A.S., and S.A. designed research; J.H. performed research; S.A. analyzed data; and J.H., J.D.L., A.S., and S.A. wrote the paper.

Reviewers: M.L., Wright State University; and P.Z., Weill Cornell Medical College.

The authors declare no conflict of interest.

Freely available online through the PNAS open access option.

Data deposition: The data reported in this paper have been deposited in the Gene Expression Omnibus (GEO) database, www.ncbi.nlm.nih.gov/geo (accession no. GSE82213).

[1]To whom correspondence may be addressed. Email: aziz_sancar@med.unc.edu or sheeraa@ekmd.huji.ac.il.

This article contains supporting information online at www.pnas.org/lookup/suppl/doi:10.1073/pnas.1614430113/-/DCSupplemental.

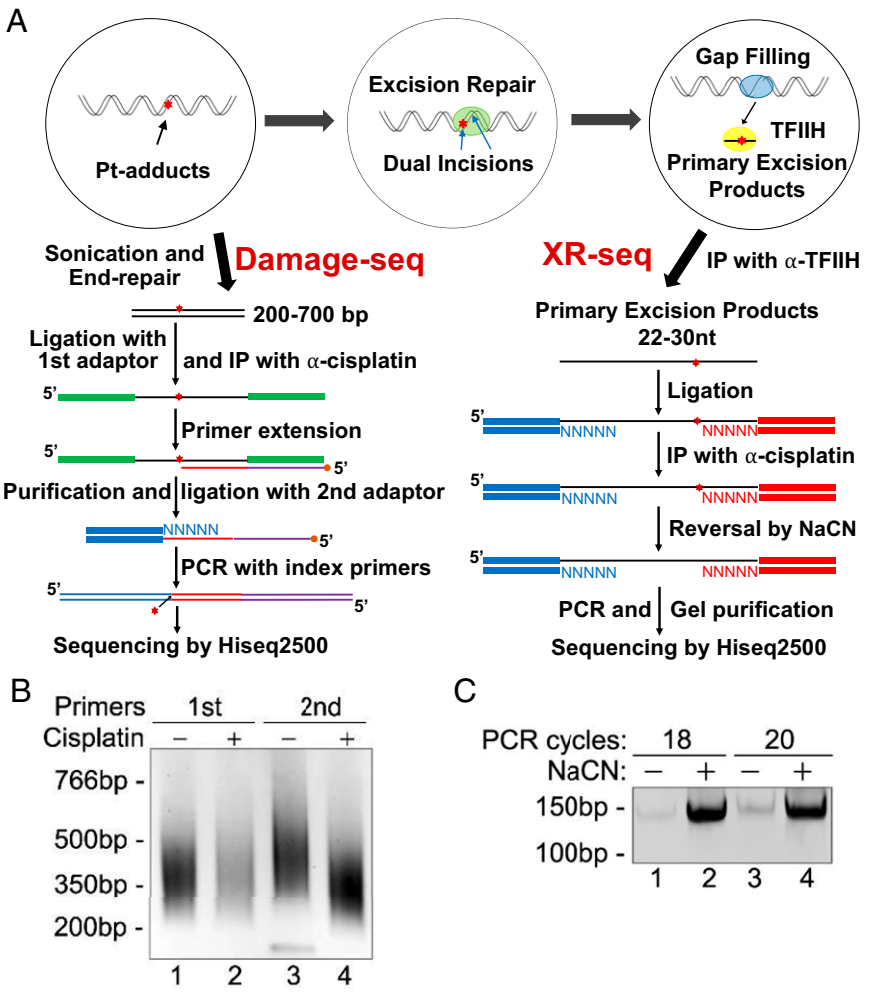

Fig. 1. Damage-seq and XR-seq methods. (*A*) Schematic representation of the methods. Red stars indicate the Pt-DNA adducts. In Damage-seq (*Left*), after damage induction, genomic DNA was sonicated and subjected to end repair. Then these end-repaired fragments (black) were ligated to the first adapters (green). This step was followed by denaturation and IP with an antibody against cisplatin adducts. Next, a biotinylated primer (purple) was annealed and extended by a DNA polymerase, which was blocked by DNA damage. The extension products (red) were purified and ligated to the second adapter (blue). Finally, the ligation products were amplified with index primers and sequenced. In XR-seq (*Right*), the 22- to 30-nt-long oligomers generated by nucleotide excision repair (black) were captured by IP with TFIIH antibodies and followed by ligation with adapters on both ends (blue and red). Then, the ligation products were purified by IP with the anti-cisplatin antibody, and the Pt adducts were reversed by incubation with NaCN. Finally, the oligomers were amplified and sequenced. For clarity, in both Damage-seq and XR-seq, the lengths of the DNA fragments and adapters are not drawn to scale. (*B*) Representative agarose gel analysis of Damage-seq libraries. DNA fragments from control and cisplatin-treated cells were amplified with sets of primers complementary to the first and second adapters. (*C*) Representative native polyacrylamide gel electrophoresis of XR-seq libraries (1% of material) showing cisplatin adduct reversal by NaCN is necessary for PCR amplification of sequencing libraries.

reads from undamaged DNA, which began with the 5′ sequence of the first adapter, were discarded before alignment and data analysis.

Cisplatin DNA eXcision Repair (XR-seq) Map. An XR-seq library for cisplatin damage was prepared by adapting the XR-seq method we previously developed for UV damage to cisplatin damage repair (13–15), with modifications in the steps of damage-specific immunoprecipitation and in vitro damage reversal (Fig. 1*A*, *Right*): After cisplatin treatment, primary excision products were pulled down by transcription factor IIH (TFIIH) coimmunoprecipitation and ligated to adapters on both ends. This step was followed by immunoprecipitation with cisplatin-specific antibodies (16). The Pt-DNA adducts in the immunoprecipitated oligomers were reversed by incubating in NaCN (5–8). Then, the oligomers were amplified by PCR to obtain the XR-seq high-throughput sequencing library (Fig. 1*C* and *SI Appendix*, Fig. S2*B*). The reads were then aligned to the human genome to generate the XR-seq map for cisplatin-induced repair of the human genome.

Cisplatin Damage-seq and XR-seq Products. Cisplatin mainly forms Pt-d(GpG) and, to a lesser extent, Pt-d(ApG), Pt-d(GpXpG) intrastrand diadduct, and at a lower frequency, Pt-G-G interstrand cross-links (2–4). According to the Damage-seq procedure (Fig. 1*A*), the cisplatin lesion should be at the nucleotides immediately 5′ (upstream) of our reads. Thus, when we aligned the filtered reads to the human genome, it was expected that the dinucleotides 5′ upstream will be diguanines (G-G and, to a lesser extent, A-G). In agreement with the prediction, G-G was highly enriched 5′ to the read start with cisplatin damaged DNA but not with undamaged DNA (Fig. 2 *A* vs. *C*, and *SI Appendix*, Fig. S3 and Table S1). Moreover, we uncovered a preference for A 5′ to the G-G dinucleotides of our Damage-seq reads (Fig. 2 *B* vs. *D* and *SI Appendix*, Fig. S4).

XR-seq for cisplatin-damaged cells revealed oligonucleotide-length distribution essentially identical to that observed with UV

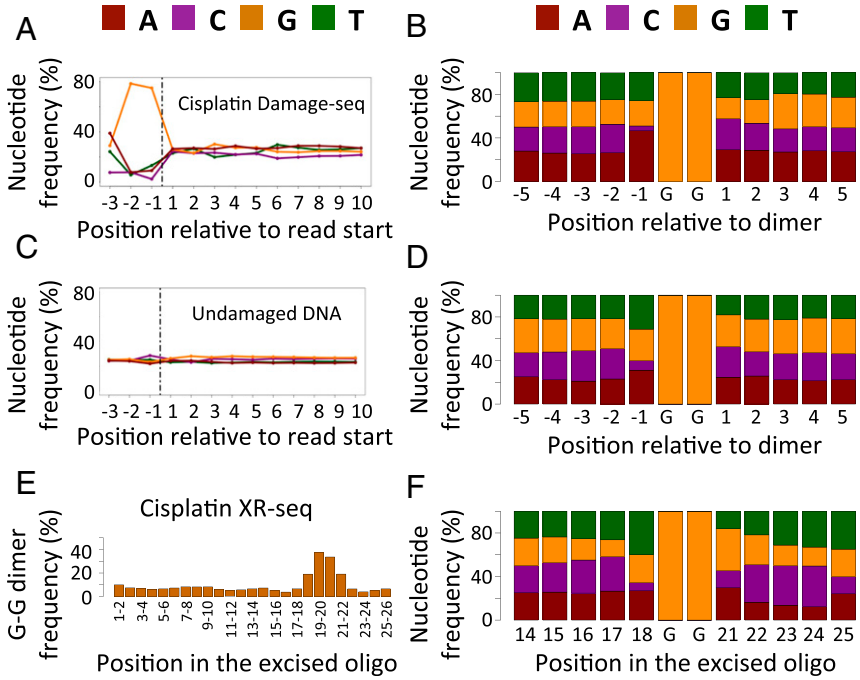

Fig. 2. Single-nucleotide resolution of cisplatin damage and repair. (*A*) Nucleotide frequencies are plotted for positions 3 nt upstream of the read start and 10 nt into the read for cisplatin Damage-seq. (*B*) Sequence context for the 5 nt flanking the most common dinucleotide associated with Pt damage. (*C* and *D*) Same as *A* and *B* except plotted are results for sequenced undamaged control DNA. (*E*) Frequency of the G-G dinucleotide at each position of 26-nt-long XR-seq excision fragments. (*F*) Nucleotide frequencies at the 5-nt flanking G-Gs at positions 19–20. Figures depict data from a representative experiment.

photoproducts with 26- to 27-nt-long excision products predominating (*SI Appendix*, Fig. S7) (5–8, 17). In contrast to the excision products of UV damage, the cisplatin XR-seq products contained G-G at ~20 nt from the 5′ and 5–6 nt from the 3′ end of the 26-nt-long excised oligomer (Fig. 2*E* and *SI Appendix*, Fig. S6*A* and Table S2), consistent with the fact that Pt-d(GpG) is the predominant DNA adduct of cisplatin. This location of the adduct indicates that regardless the type of damage (UV or cisplatin-induced lesions), the dual incision sites characteristic of nucleotide excision repair (17) are virtually the same. In

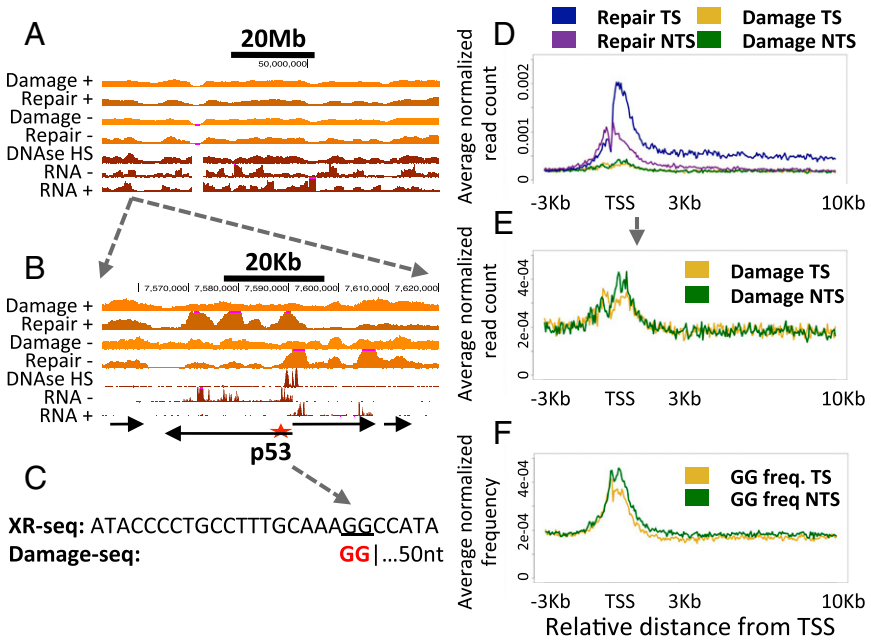

Fig. 3. Genome-wide patterns of damage and repair of cisplatin damage. (*A*) Representative screen shot of damage and repair signals, separated by strand, for the entire chromosome 17. (*B*) Zoom-in on *A* ~80-kbp segment of chromosome 17, which includes TP53. (*C*) Representative XR-seq and Damage-seq reads that capture a specific Pt-d(GpG) damage. (*D*) Damage and repair profiles of the transcribed and nontranscribed strands surrounding TSS of highly expressed genes. (*E*) Zoomed-in scale for the damage levels. (*F*) Same as *E* except plotted are GG frequencies on each strand. Data normalized per million mapped reads or million counted GGs. Figures represent data from merged replicates.

contrast to Damage-seq, there was a preference for T 5′ and G 3′ of the G-G dinucleotides in XR-seq reads (Fig. 2*F* and *SI Appendix*, Fig. S6*B*), indicating a possible sequence context preference for excision. We cannot discriminate whether these G-G-G sequences are a sequence context preference for Pt-d(GpG) excision or excision of Pt-d(GpXpG).

Genome-Wide Maps of Cisplatin Damage and Repair. Our ability to map damage and repair genome-wide provided the data necessary to examine the determinants of damage sensitivity throughout the genome (Fig. 3 *A*–*C* and *SI Appendix*, Fig. S7–S9). As an example, we focused on chromosome 17, which carries the *TP53* gene that is mutated in approximately 50% of human cancers. We followed repair from a chromosome-wide scale (Fig. 3*A*) to a more focused gene-centric analysis (Fig. 3*B*) and, finally, to single nucleotides at a specific cisplatin-d(GpG) damage site in *TP53* that was captured by representative Damage-seq and XR-seq reads (Fig. 3*C*).

As apparent from the high-resolution data, whereas cisplatin damage distribution was essentially uniform the repair efficiency was rather heterogeneous. This difference was particular striking when damage and repair of Pt adducts in the transcribed strand of *TP53* were compared.

To analyze the effect of transcription on damage and repair genome-wide, we plotted damage and repair levels surrounding the transcription start sites (TSS; Fig. 3 *D* and *E*) and transcription end sites (TES; *SI Appendix*, Fig. S10) of highly expressed genes in GM12878 cells (11). Similar to CPD repair (18, 19), cisplatin repair was transcription coupled, with higher repair of the transcribed strand, starting from TSS and continuing up to the TES. In comparison with the repair levels, damage levels appeared virtually uniform. However, upon close inspection at high resolution we did observe subtle differences in damage levels at the starts and ends of genes (Fig. 3*E* and *SI Appendix*, Fig. S10): Pt damage was slightly enriched over the TSS and slightly depleted over the TES. To determine whether this enrichment was due to the unique features of TSS or a simple reflection of the cisplatin target dinucleotide sequence frequencies, we analyzed G-G frequency in the TSSs of the same group of genes: The G-G frequency at TSS and TES mirrored the Pt-d(GpG) damage (Fig. 3*F* and *SI Appendix*, Fig. S10).

Effect of Nucleosome and Chromatin States on Damage Formation and Repair. To detect possible effects of nucleosome occupancy on damage formation and repair, we used existing nucleosome mapping data from GM12878 (11) and plotted damage levels surrounding the center of nucleosome positions. We observed a distinct periodicity of damage formation surrounding the center position of nucleosomes ("in vivo", Fig. 4*A*). However, a similar periodicity was observed when we plotted damage formation in cisplatin-treated naked DNA ("in vitro") or the frequency of the

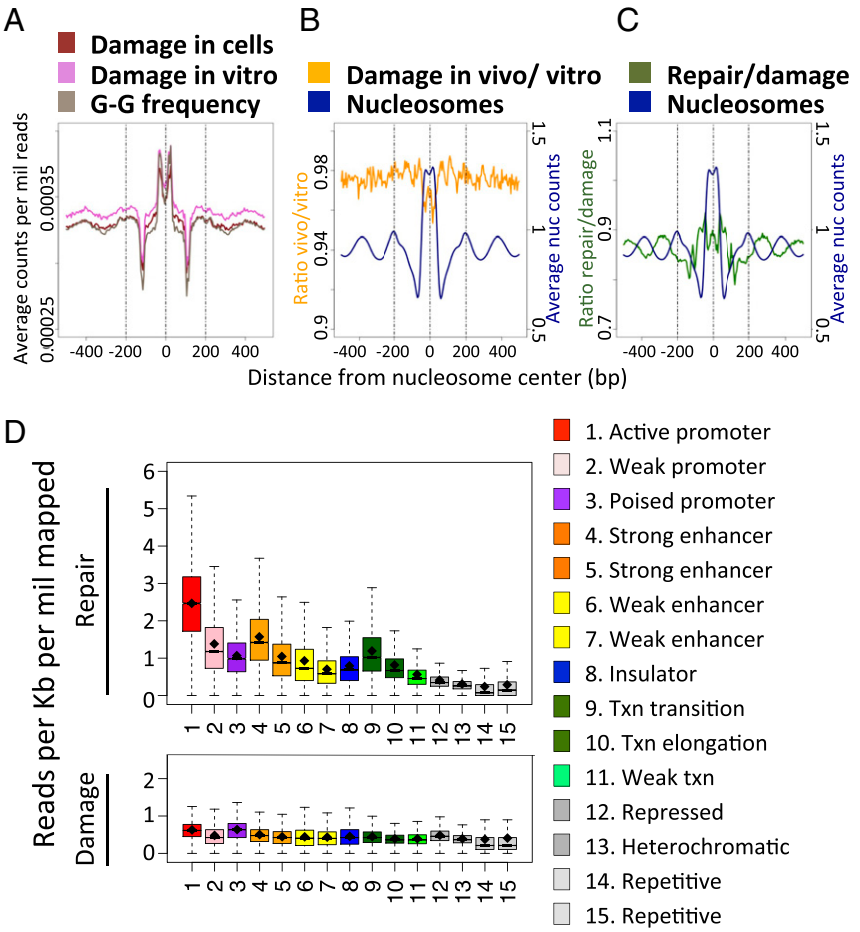

Fig. 4. Effect of nucleosomal location and chromatin states on cisplatin damage formation and repair. (*A*) Average in vivo Damage-seq (red), in vitro Damage-seq (pink), and the relevant dinucleotide frequency (gray) at 1 Kbp flanking the center of nucleosomes in GM12878 cells. (*B*) Similar to *A*, except plotted is ratio of in vivo to in vitro cisplatin damage. Mnase-seq nucleosomal signal is plotted for comparison. (*C*) Similar to *B*, except plotted is the ratio of repair to damage. (*D*) Analysis of repair (*Upper*) and damage (*Lower*) levels across the 15 annotated chromatin states of GM12878 for cisplatin damage reveals uniform distribution of damage but higher repair levels in open regions in the genome. Figures represent data from merged replicates.

G-G dinucleotide, indicating that the damage periodicity simply reflects the periodicity of the target dinucleotide. In Fig. 4*B*, we plot the ratio of cisplatin damage in vivo to in vitro at the same positions. We see a slight dip in the ratio at the nucleosome centers, indicating that adduct formation near the nucleosome center was inhibited, albeit at a level of ∼5% relative to other positions.

In contrast to damage formation, Fig. 4*C* shows that repair efficiency exhibited periodicity that was antiphase with the nucleosome center, which is consistent with nucleosomes making cisplatin DNA adducts refractory to repair (8). These results agree with the observation that repair is strongly associated with DNase-HS sites (*SI Appendix*, Fig. S11 and refs. 13 and 14), whereas damage levels are relatively uniform.

Finally, we analyzed the association of 15 chromatin states with DNA repair. The chromatin states are derived from histone posttranslational modifications and genomic sequence elements, with functional roles inferred for each state (20). We found that similar to the repair of UV damage [CPD and (6, 4)photoproducts] (13, 14), Pt-damage repair was higher in active chromatin states such as active promoters and strong enhancers (Fig. 4*D* and *SI Appendix*, Fig. S12*A*, *Top*). In stark contrast, the distribution of the damages, with some minor differences, was rather uniform (Fig. 4*D* and *SI Appendix*, Fig. S12*A*, *Bottom*). The subtle differences in damage frequency that were observed as a function of genomic position followed differences in the underlying frequencies of the relevant dinucleotide, d(GpG) (*SI Appendix*, Fig. S12*B*).

Discussion

Although cisplatin and its second- and third-generation derivatives have been used for decades with considerable success in cancer management (1–4), some cancers exhibit primary or acquired resistance limiting its general usefulness. Because cisplatin-induced DNA damage is repaired by nucleotide excision repair, the role of this repair mechanism in cisplatin efficacy or resistance needs to be delineated. Previous studies have used global genome repair assays to address this issue but the results have been inconclusive (1–8). High resolution maps of DNA damage formation and repair would aid in understanding the genomic variables that affect sensitivity to genotoxic agents. Methods for mapping cisplatin (21) and UV (21–26) damage in yeast and human cells have been described. However, whereas CPDs can be mapped at high resolution (22, 25), the utility of mapping of cisplatin has been limited because of the low resolution and the lack of strandedness. Moreover, these maps were not accompanied with the corresponding repair maps, which are necessary for making extrapolations vis a vis damage location-repair-biological end points.

Here, we present methods for single-nucleotide resolution mapping of cisplatin damage and repair. We show that cisplatin-induced DNA damage is essentially uniformly distributed in the human genome, and damage incidence is dictated primarily by the underlying G-G frequency. This finding is in agreement with a previous low-resolution study that mapped cisplatin and oxaliplatin damage (21). Comparing in vivo and in vitro damage formation at nucleosomes indicates nucleosome binding affords a small degree of protection from cisplatin damage formation. We do not observe the strong effect of nucleosome rotational setting on damage formation as was reported for CPDs in a recent high-resolution study in yeast (25). This observation may be due to an inherent difference between cisplatin and UV damage formation, or between yeast and human nucleosome organization. We cannot rule out, however, that compared with the yeast study, which used high-resolution nucleosome positions, the nucleosome mapping available for GM12878 is less accurate. Less accurate positions would compromise our ability to precisely measure damage formation relative to the nucleosome centers, and the protection may be higher than we report.

In stark contrast to damage formation, the efficiency of repair is highly heterogeneous and significantly correlated to transcription and chromatin states. Thus, the overall effect of damages in the human genome is primarily driven by the repair efficiency and not by damage formation. Cisplatin resistance, primary or acquired, is multifactorial likely encompassing uptake, efflux, drug inactivation by sulfhydryl groups, and finally repair. We believe that the single-nucleotide resolution methods for cisplatin damage and repair we have described in this paper should aid in determining the contribution of repair to cisplatin efficacy or resistance as our previous XR-seq data has for UV mutagenesis (14, 27, 28). This goal will require the generation of damage and repair maps in cancers from different tissues. Then, it would be possible to develop rational approaches to overcome cisplatin resistance and improve the efficacy of cisplatin treatment. We note that the Pt-based drugs form interstrand cross-links at low frequency (1–4). Our method, in its present form, does not detect the formation and repair of these damages. However, it is generally accepted that these rare interstrand cross-links do not substantially contribute to Pt drug efficiency and toxicity. Finally, we note that Damage-seq should be applicable to the study of damage and repair of other carcinogens and chemotherapeutic drugs.

Materials and Methods

Human lymphocyte cell line GM12878 was grown to ∼8×10^5 cells per mL before treatment. For Damage-seq and XR-seq, cells were incubated in media containing 200 μM cisplatin or oxaliplatin for 1.5 and 3 h, respectively. Damage-seq detected Pt-adducts based on the blockage of DNA polymerase in vitro by damage. Pt-XR-seq was modified from UV-XR-seq. (13). Detailed description of the methods and data analysis is found in *SI Appendix, SI Materials and Methods*.

ACKNOWLEDGMENTS. We thank Dr. Sebastian Pott for fruitful discussion and advice. This work was supported by NIH Grant GM118102.

1. Kelland L (2007) The resurgence of platinum-based cancer chemotherapy. *Nat Rev Cancer* 7(8):573–584.
2. Wang D, Lippard SJ (2005) Cellular processing of platinum anticancer drugs. *Nat Rev Drug Discov* 4(4):307–320.
3. Hall MD, Okabe M, Shen DW, Liang XJ, Gottesman MM (2008) The role of cellular accumulation in determining sensitivity to platinum-based chemotherapy. *Annu Rev Pharmacol Toxicol* 48:495–535.
4. Jamieson ER, Lippard SJ (1999) Structure, recognition, and processing of cisplatin-DNA adducts. *Chem Rev* 99(9):2467–2498.
5. Reardon JT, Vaisman A, Chaney SG, Sancar A (1999) Efficient nucleotide excision repair of cisplatin, oxaliplatin, and Bis-aceto-ammine-dichloro-cyclohexylamine-platinum(IV) (JM216) platinum intrastrand DNA diadducts. *Cancer Res* 59(16):3968–3971.
6. Huang JC, Zamble DB, Reardon JT, Lippard SJ, Sancar A (1994) HMG-domain proteins specifically inhibit the repair of the major DNA adduct of the anticancer drug cisplatin by human excision nuclease. *Proc Natl Acad Sci USA* 91(22):10394–10398.
7. Zamble DB, Mu D, Reardon JT, Sancar A, Lippard SJ (1996) Repair of cisplatin–DNA adducts by the mammalian excision nuclease. *Biochemistry* 35(31):10004–10013.
8. Wang D, Hara R, Singh G, Sancar A, Lippard SJ (2003) Nucleotide excision repair from site-specifically platinum-modified nucleosomes. *Biochemistry* 42(22):6747–6753.
9. Wood RD (1997) Nucleotide excision repair in mammalian cells. *J Biol Chem* 272(38): 23465–23468.
10. Reardon JT, Sancar A (2005) Nucleotide excision repair. *Prog Nucleic Acid Res Mol Biol* 79:183–235.
11. ENCODE Project Consortium (2012) An integrated encyclopedia of DNA elements in the human genome. *Nature* 489(7414):57–74.
12. Vaisman A, et al. (1999) Effect of DNA polymerases and high mobility group protein 1 on the carrier ligand specificity for translesion synthesis past platinum-DNA adducts. *Biochemistry* 38(34):11026–11039.
13. Hu J, Adar S, Selby CP, Lieb JD, Sancar A (2015) Genome-wide analysis of human global and transcription-coupled excision repair of UV damage at single-nucleotide resolution. *Genes Dev* 29(9):948–960.
14. Adar S, Hu J, Lieb JD, Sancar A (2016) Genome-wide kinetics of DNA excision repair in relation to chromatin state and mutagenesis. *Proc Natl Acad Sci USA* 113(15):E2124–E2133.
15. Hu J, et al. (2013) Nucleotide excision repair in human cells: Fate of the excised oligonucleotide carrying DNA damage in vivo. *J Biol Chem* 288(29):20918–20926.
16. Liedert B, Pluim D, Schellens J, Thomale J (2006) Adduct-specific monoclonal antibodies for the measurement of cisplatin-induced DNA lesions in individual cell nuclei. *Nucleic Acids Res* 34(6):e47.

17. Huang JC, Svoboda DL, Reardon JT, Sancar A (1992) Human nucleotide excision nuclease removes thymine dimers from DNA by incising the 22nd phosphodiester bond 5′ and the 6th phosphodiester bond 3′ to the photodimer. *Proc Natl Acad Sci USA* 89(8):3664–3668.
18. Mellon I, Spivak G, Hanawalt PC (1987) Selective removal of transcription-blocking DNA damage from the transcribed strand of the mammalian DHFR gene. *Cell* 51(2):241–249.
19. Hanawalt PC, Spivak G (2008) Transcription-coupled DNA repair: Two decades of progress and surprises. *Nat Rev Mol Cell Biol* 9(12):958–970.
20. Ernst J, et al. (2011) Mapping and analysis of chromatin state dynamics in nine human cell types. *Nature* 473(7345):43–49.
21. Powell JR, et al. (2015) 3D-DIP-Chip: A microarray-based method to measure genomic DNA damage. *Sci Rep* 5:7975.
22. Bryan DS, Ransom M, Adane B, York K, Hesselberth JR (2014) High resolution mapping of modified DNA nucleobases using excision repair enzymes. *Genome Res* 24(9):1534–1542.
23. Zavala AG, Morris RT, Wyrick JJ, Smerdon MJ (2014) High-resolution characterization of CPD hotspot formation in human fibroblasts. *Nucleic Acids Res* 42(2):893–905.
24. Teng Y, et al. (2011) A novel method for the genome-wide high resolution analysis of DNA damage. *Nucleic Acids Res* 39(2):e10.
25. Mao P, Smerdon MJ, Roberts SA, Wyrick JJ (2016) Chromosomal landscape of UV damage formation and repair at single-nucleotide resolution. *Proc Natl Acad Sci USA* 113(32):9057–9062.
26. Yu S, et al. (July 28, 2016) Global genome nucleotide excision repair is organised into domains that promote efficient DNA repair in chromatin. *Genome Res*, 10.1101/gr.209106.116.
27. Sabarinathan R, Mularoni L, Deu-Pons J, Gonzalez-Perez A, López-Bigas N (2016) Nucleotide excision repair is impaired by binding of transcription factors to DNA. *Nature* 532(7598):264–267.
28. Perera D, et al. (2016) Differential DNA repair underlies mutation hotspots at active promoters in cancer genomes. *Nature* 532(7598):259–263.